Cooperative formation of long-range ordering in water ad-layers on $Fe_3O_4(111)$

Francesca Mirabella,[1,#] Eman Zaki,[1,#] Francisco Ivars-Barceló, [1] Xiaoke Li, [2,#] Joachim Paier, [2]* Joachim Sauer,[2] Shamil Shaikhutdinov,[1]* Hans-Joachim Freund[1]

[1]*Fritz-Haber-Institute, Max Planck Society, Faradayweg 4-6, 14195 Berlin, Germany*

[2]*Institut für Chemie, Humboldt Universität zu Berlin, 10099 Berlin, Germany*

Abstract

The initial stages of water adsorption on magnetite $Fe_3O_4(111)$ surface and the atomic structure of the water/oxide interface remain controversial. Herein, we provide experimental results obtained by infrared reflection-absorption spectroscopy (IRAS) and temperature programmed desorption (TPD), corroborated by density functional theory (DFT) calculations showing that water readily dissociates on Fe_{tet} sites to form two hydroxo species. These act as an anchor for water molecules to form a dimer complex which self-assembles into an ordered (2×2) structure. Water ad-layer ordering is rationalized in terms of a cooperative effect induced by a hydrogen bonding network.

Keywords: iron oxides; magnetite; surface structures; water adsorption; density functional theory.

* Corresponding authors: shaikhutdinov@fhi-berlin.mpg.de
joachim.paier@chemie.hu-berlin.de

[#] These authors equally contributed to the work.

Water interaction with oxide surfaces plays an important role in geology, electrochemistry, corrosion, water splitting, catalysis, etc.[1] Iron oxides, in particular magnetite (Fe_3O_4), are some of the most studied oxides using a "surface science" approach.[2] We will provide the first compelling experimental and theoretical evidence that on the Fe_3O_4(111) surface water adsorption leads to cooperative adsorption of dissociated and molecular water species, which induces the formation of an ordered water monolayer, monitored via structural and spectroscopic studies in combination with density functional theory (DFT) calculations.

While recent experimental and theoretical work on the structure of Fe_3O_4(001) single crystal surfaces suggest that it is well-understood,[2b] the (111) surface remains controversial for. On the basis of structural studies also corroborated by DFT calculations, a single metal (namely, Fe_{tet1}-) termination is considered as the most stable,[3] whereas a double metal (Fe_{oct2}-Fe_{tet1}) termination was favored on the basis of CO and water adsorption studies using infrared reflection absorption spectroscopy (IRAS).[4] Our recent study[5] seems to have eliminated such a discrepancy by employing DFT calculations for CO adsorption. The combined experimental and theoretical results could only be rationalized in terms of the Fe_{tet1}-terminated Fe_3O_4(111) surface, although octahedrally coordinated iron ions as minority species may be present at surface defects. Note that, in contrast to CO that adsorbs intact under UHV-based conditions and has, therefore, been used as a probe molecule for surface termination, water readily dissociates on the Fe_3O_4(111) surface,[2a, 6] thus rendering determination of the surface termination by water adsorption difficult. Indeed, it was generally accepted that a water molecule dissociates on Fe_{tet1}-terminated Fe_3O_4(111) ultimately forming two surface hydroxo species, i.e. Fe-O_wH and O_sH (where O_w and O_s label oxygen atoms in water and oxide surface, respectively). [6-7] However, this scenario was questioned by results presented in ref.[4b] suggesting spontaneous formation of a complex composed of dissociated and non-dissociated water molecules (a so-called "half-dissociated" water dimer) based on the assumption, however, that the surface is Fe_{oct2} –terminated.

In order to provide a unified picture for the structure and adsorption properties of the Fe_3O_4(111) surface, in this work we re-examined water adsorption models. Using well-characterized Fe_3O_4(111) thin film surfaces and taking careful precautions with respect to the film preparation and surface termination, we show that all experimental results agree

well with the „classical“ dissociation mechanism resulting in a terminal (Fe-O_wD) hydroxyl and surface hydroxyl O_sD at the initial stage. Analysis of the previous studies on Fe_3O_4(111), both for single crystals and thin films, suggests that a certain controversy that exists in the literature may have resulted from the experimental difficulties of preparing well-defined, clean and uniform surfaces. In particular, single crystal studies may suffer from having several surface structures coexisting. Although thin films grown on a metal substrate appear to be uniform, defect structures are still difficult to control and characterize. In addition, surface preparation and even vacuum conditions may play an important role due to adventitious adsorption of residual gases in the background. Finally, from a theoretical point of view, adsorption on iron oxide systems needs careful consideration as far as electronic and magnetic properties are concerned (see ref. [4c] and references therein).

In this work, we used well-ordered Fe_3O_4(111) thin films grown on Pt(111) (see Experimental). Prior to water adsorption, the films were characterized by CO adsorption in the same manner as described in ref. [5] to ensure that the Fe_{tet1}-termination dominates the surface. We first address temperature programmed desorption (TPD) results. Figure 1a shows a series of TPD spectra as a function of water coverage obtained after D_2O dosing at 140 K and heating to 700 K in each run. Beyond the desorption peak at ~ 160 K assigned to the onset of the amorphous solid water (ASW) (or “ice”, for simplicity) film formation, several desorption peaks are clearly resolved at 201, 223, and 255 K which are sequentially populated at increasing exposure. The peak positions are independent of water coverage, indicating a first order desorption kinetics. In contrast, a broad signal above 270 K shows typical behavior for second order kinetics expected for recombinative desorption of dissociated water.[6c] Finally, a small signal at around 375 K, which may even be saturated by reaction with residual water in UHV during cooling the sample to 140 K, can safely be assigned to adsorption on defect sites.

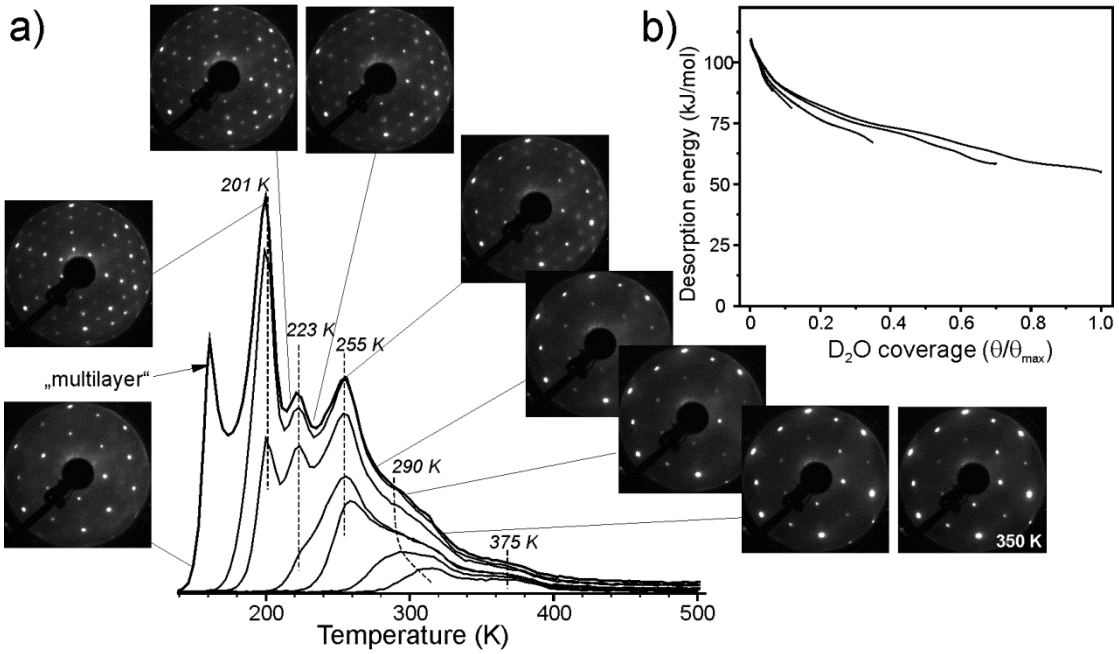

Figure 1. (a) TPD spectra of D_2O adsorbed at 140 K at increasing exposures. The spectra are cut at 500 K, for clarity. At the highest exposure, the formation of "multilayer" (ASW) film sets in. The heating rate is 3 K/s. Snapshots from the LEED (E = 64 eV) movie recorded while heating the sample covered by the ASW film at 140 K synchronized with a TPD spectrum. (b) Desorption energy as a function of water coverage, normalized to the total coverage (θ_{max}) measured before ASW formation, obtained by inversion analysis of the Polanyi-Wigner equation applied to each spectrum shown in (a), see text.

The desorption spectra can be transformed into coverage dependent desorption energy plots using inversion analysis of the well-known Polanyi-Wigner equation.[8] For first order desorption kinetics this procedure yields the desorption energies (*E*) as a function of water coverage (θ): $E(\theta) = -RT \ln\left[-\frac{d\theta/dT}{\beta \nu \theta}\right]$ where β is a heating rate, and ν is a pre-factor. Figure 1b shows the results for $\nu = 10^{13}$ s^{-1} commonly used. Although the absolute values depend on the pre-factor (increasing the pre-factor to 10^{15} s^{-1} leads to a shift of all energies towards higher (i.e. more exothermic) values by about 15 kJ/mol), the results clearly show that the desorption energy considerably decreases with increasing coverage, most markedly in the low coverage regime ($\theta/\theta_{max} < 0.15$), in nice agreement with microcalorimetry results.[4b]

To quantify water coverage, we made use of TPD spectra on the clean Pt(111) surface showing a characteristic desorption feature upon formation a well-ordered ice film.[9] Since the measurements were performed with the same setup and on the same Pt crystal as used for the iron oxide film, all apparatus effects are self-cancelled. The results showed that the total amount of water adsorbed on Fe_3O_4(111) before the ASW film starts to grow, corresponds to 2.3 ± 0.2 ML (1 ML is defined as 3.2×10^{14} cm^{-2}, i.e. one water

molecule per Fe_3O_4(111) unit cell). This value agrees fairly well with the model of a half-dissociated water dimer (i.e. two H_2O per unit cell) forming at increasing water coverage, previously put forward by Joseph et al. [6a]. However, their TPD spectra (see also refs. [6c, 7b]) showed, in essence, featureless desorption traces in the 200 – 300 K region. Such a picture is often attributed to surface heterogeneity and/or reorganization of ad-species during the TPD run, thus broadening and smearing desorption features. In contrast, the presence of well-resolved peaks in our spectra favor the model where each desorption peak showing first order kinetics is associated with individual desorption of water molecules having discrete binding energies. In principle, this could be the case when several adsorption sites coexist on the surface, from which water desorbs independently. Such an explanation was essentially provided in refs. [7c, 10] reporting TPD peaks of water on the Fe_3O_4(111) selvedge surface of a hematite Fe_2O_3(0001) natural crystal, since different surface phases are inevitably formed during surface preparation. This is obviously not the case for our films exposing a single termination.

Under the assumption that the TPD signal at high temperatures above ~ 270 K is associated with dissociated water, the observation of three distinct desorption peaks at 200 – 255 K is difficult to rationalize within a simple dimer model having only one non-dissociated water molecule per unit cell. Therefore, this finding suggests the formation of water oligomers larger than a dimer (e.g. trimer and tetramer). Alternatively, three-dimensional water clusters are formed, from which water molecules desorb in a one-by-one manner. Sharp desorption signals imply species desorbing almost simultaneously, suggesting, in turn, a certain degree of ordering at the surface.

To examine whether water forms ordered structures on Fe_3O_4(111) we employed low energy electron diffraction (LEED). Certainly, careful precautions had to be taken in order to minimize electron beam damaging effects. Figure 1a displays snapshots from the LEED movie recorded upon heating of the ASW film (formed by 1.5 L D_2O at 140 K) to synchronize with the thermal desorption. Additional spots clearly identified as of Fe_3O_4(111)-(2×2) appear upon desorption of the ASW film and attenuates above ~ 260 K. The formation of the (2×2) structure depends on the water coverage and not on the adsorption temperature (140 K vs 250 K). The latter finding indicates that ordering is thermodynamically driven and not kinetically limited. Note also, that the (2×2) spots appear in LEED immediately upon electron beam exposure and showed no intensity attenuation in

time, at least, on the scale of a minute. Rapidly changing the spot position for sampling also showed no effect on the LEED spots intensity. Therefore, we can safely rule out beam effects on water ordering.

There are only a few examples in the literature on water/oxide interfaces which exhibited an ordered water ad-layer.[11] Water adsorption on the MgO(001) surface is likely the most intensively studied system (ref.[12] and references therein) that showed *c*(4×2) and *p*(3×2) structures in LEED.[13] Using a genetic algorithm, DFT calculations predicted two stable structures. At low temperature, a *c*(4×2) structure is stable that contains ten water molecules in the cell thus leading to a nominal coverage 1.25 H_2O per MgO(001) unit cell. A *p*(3×2) structure containing six water molecules per cell (1 H_2O per surface cell) is more stable at high temperature. Both structures feature surface hydroxyl groups resulting from the dissociation of water molecules. However, the way these structures form on MgO(001) remains poorly understood. In the case of adsorption on ZnO(10-10),[11a] the dissociation only occurs when two molecules occupy adjacent adsorption sites thus resulting in a half-dissociated dimer forming a (2×1) superstructure.

To shed light on the atomic structure of the water ad-layer on Fe_3O_4(111), we performed IRAS measurements. Full analysis will be presented in a forthcoming paper;[14] here we only highlight key observations. Figure 2a shows a series of spectra obtained at the saturating exposure at the sample temperature as indicated. A sharp band at 2680 cm^{-1} appears at 350 K and almost doubles intensity upon water dosing at 320 and 300 K. At increasing coverage achieved by water exposure at 250 K, the band at 2723 cm^{-1} signal gains considerable intensity, and the peak shifts to 2714 cm^{-1}. Concomitantly, a new band at 2688 cm^{-1} grows, whereas the band at 2680 cm^{-1} disappears. In addition, a weak band shows up at 2565 cm^{-1} which falls in the range of hydrogen bonding OD species. At 200 K, two bands, at 2710 and 2693 cm^{-1}, start to dominate the spectrum in this region, while very broad signals develop in the 2650 – 2450 cm^{-1} region indicating the formation of a hydrogen bonding network, culminating in the formation of the ASW film at 120 K. The latter shows a well-known band at 2726 cm^{-1} assigned to a “dangling” OD vibration at the water surface and a broad band centered at 2580 cm^{-1} of hydrogen bonded OD species in the bulk.

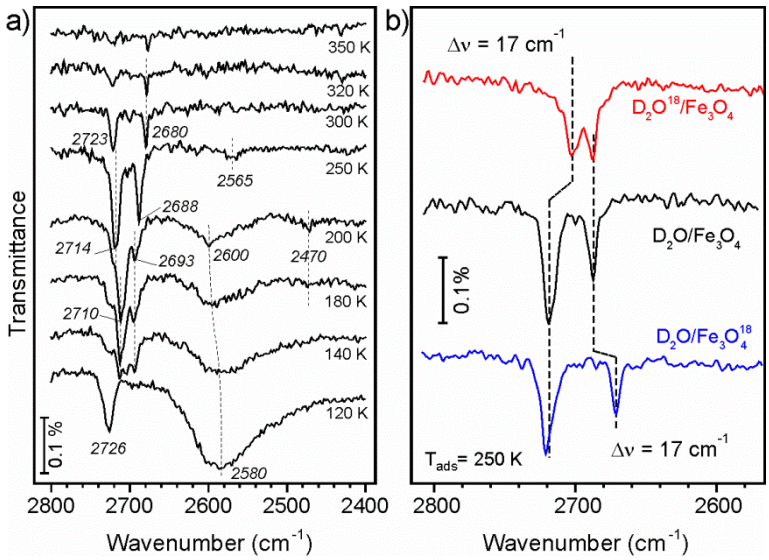

Figure 2. (a) IRA spectra obtained at the saturating exposure at the sample temperature as indicated (see text). (b) IRA spectra obtained at 250 K for ^{18}O- labelled water (red) and oxide film (blue) for comparsion with results on D_2O/Fe_3O_4(111) shown in panel (a).

The band around 2720 cm^{-1} falls in the range calculated by DFT[4b, 4c] for stretching vibrations of terminal O_wD hydroxyl formed by dissociation of a single water molecule on both surface terminations, i.e. 2754 cm^{-1} on Fe_{oct2}- and 2729 cm^{-1} on Fe_{tet1}-terminated surfaces, when scaled using observed fundamentals of the water molecule (see ref. [4b]). However, computed frequencies for surface hydroxyls (O_sD) considerably differ and are expected to show up at ~ 2440 cm^{-1} and 2705 cm^{-1}, for the Fe_{oct2}- and Fe_{tet1}- termination, respectively. To further identify the nature of the observed sharp bands in the 2720 – 2680 cm^{-1} region with the help of isotopic labelling, we performed adsorption experiments with $D_2{}^{18}O$ water on the same film. In addition, "normal" D_2O water was exposed to the oxide film prepared with ^{18}O. The results of adsorption at 250 K are summarized in Fig. 3b for direct comparison with D_2O/Fe_3O_4(111). Clearly, only the band at 2714 cm^{-1} red-shifts upon $D_2{}^{18}O$ adsorption, whereas the 2688 cm^{-1} band only shifts upon ^{18}O labeling in the oxide, both shifts being about 17 cm^{-1}. Therefore, the high frequency bands above 2710 cm^{-1} must be associated with terminal Fe-O_wD, and the bands below 2695 cm^{-1} - with surface hydroxyls O_sD, in agreement with the "classical" adsorption model involving single water molecule dissociation on a cation-anion pair resulting in two hydroxyls as observed. However, these results are at variance with those previously reported in ref.[4b] showing that the bands (at 2720 and 2695 cm^{-1} in that case) are originating from water and do not involve surface oxygen. To validate our current bands assignment, we performed additional IRAS

experiments in another UHV setup on several identically prepared samples which fully reproduced the isotopic shifts as in Fig. 2b. In order to scrutinize such discrepancy, we analyzed experimental details in both studies which revealed a critical role of the surface preparation and vacuum conditions on water adsorption results especially at low coverages (only presented in ref.[4b]). It is found that UHV annealing at high temperatures (above 750 K) is important for the formation of a uniform Fe_{tet1}-terminated surface as highlighted in the I/V LEED study[3c] and also in our most recent IRAS/DFT study of CO adsorption.[5] Unfortunately, this condition was not carefully controlled in the previous water adsorption study.[4b]

The evolution of the spectra shown in Fig. 2a is rather complex and suggests a rearrangement of water species upon increasing coverage up to the critical point where long-range ordering takes place as judged by LEED. In principle, two scenarios could be envisioned. In the first one, water molecules dissociate and give rise to hydroxo species which form a (2×2) array as a template which is maintained upon adding further water molecules. It is more plausible, however, that the formation of a (2×2) structure only occurs upon molecular water adsorption. Indeed, water ordering is not observed by LEED at 300 K, i.e. in relative abundance of dissociated water species. On the other hand, it cannot be ruled out that the high coverage, only reached at low temperatures, is needed solely to be observed by conventional LEED requiring ordered structures in areas larger than 5 – 10 nm.

The formation of the (2×2) ordered structure was further analyzed on the basis of DFT calculations henceforth using a $Fe_3O_4(111)$-(2×2) supercell. Equation (1) describes the chemical reaction of sequential water adsorption:

$$Fe_3O_4(111)\cdot nH_2O + H_2O \rightleftharpoons Fe_3O_4(111)\cdot(n+1)H_2O, \qquad (1)$$

$$\Delta E(n) = E_{n+1} - (E_n + E_{H2O})$$

As previously observed for the (1×1) slabs, the first water molecule strongly adsorbs and readily dissociates (ΔE = -123 kJ/mol). The second water molecule in the cell (i.e. 0.5 ML coverage) may either dissociate on available empty Fe-O sites or anchor to the preformed hydroxyls to form a dimer (Fig. 3). Although, according to calculated energies, both processes are equally possible (-100 vs -104 kJ/mol per water molecule), the energy gain is considerably smaller than for monomer formation on the clean surface (-123 kJ/mol).

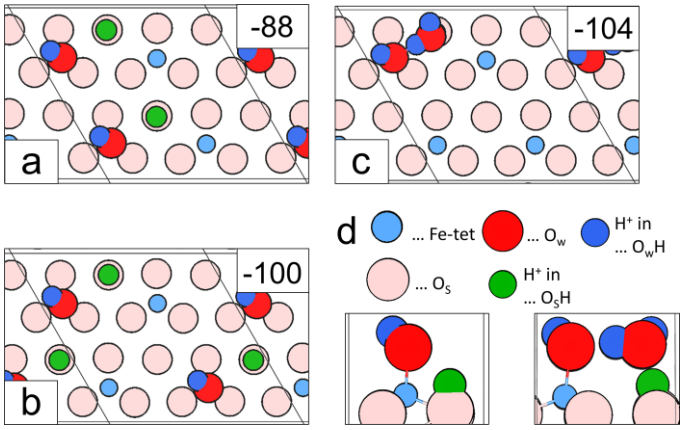

Figure 3. Top views of several computed structures containing two water molecules in the (2×2) cell. The calculated ΔE energies in kJ/mol are shown in the insets. Cross views of a "monomer" and a "dimer" are shown in (d).

Therefore, at coverages close to 1 ML (i.e. four H_2O molecules in the cell), the oxide surface is predicted to be covered primarily by hydroxyls, although dimers can also be found. In order to model structures at higher coverages, we performed calculations by adding water molecules one-by-one to a surface fully covered by monomers (= 1ML). Obviously, the first additional water molecule anchors to one of the monomers to form a dimer (not shown). The optimized structures and reaction energies ΔE for the case of 6,7 and 8 molecules per (2×2) cell are shown in Fig. 4. Note that zero point vibrational energy corrections per H_2O molecule only cause a constant shift upon calculation of reaction energies for each of the (2×2) structures considered (see Table 1 in Supporting Information). Therefore, only PBE+U total energies are used for discussion. For six H_2O molecules per cell (1.5 ML), the structure consisting of a trimer (the "clustered" structure, $\mathbf{6^{cl}}$) is more stable than of that of a dimer and a monomer forming a hydrogen bonding network ($\mathbf{6^{n}}$). However, adding one H_2O to the structure $\mathbf{6^{cl}}$ yields ΔE = -56 kJ/mol, whereas a more exothermic reaction (ΔE = -74 kJ/mol) is obtained by the formation of the "network" structure $\mathbf{7^{n}}$, where dimers start to build a 2D network by maximizing hydrogen bonds. This reaction pathway further dominates for the case of 8 H_2O molecules per cell, basically following the Bernal-Fowler rules.[15] Thus, the 2D water network formation is thermodynamically favored. Moreover, the structure $\mathbf{8^{n}}$ features a (1×1) symmetry that is in good agreement with LEED data (Fig. 1) showing a sharp (1×1) pattern at 140 K before the (2×2) structure develops. Although there is no direct proof

(e.g. by scanning tunneling microscopy) for the atomic structure of the unit cell in the network, the proposed scenario is consistent with the experimental findings.

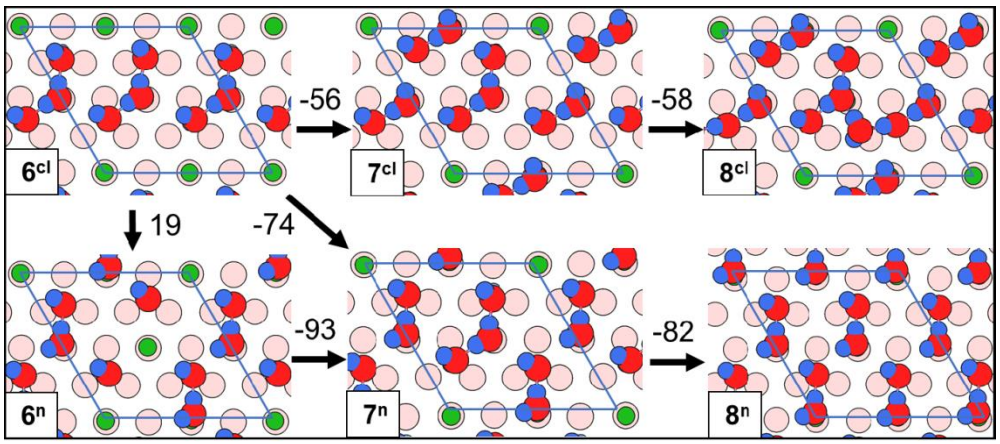

Figure 4. Top and side views of several computed structures containing 6, 7 and 8 water molecules in a Fe_3O_4(111)-(2×2) cell. The top panel depicts the formation of oligomers, and the bottom panel shows development of the hydrogen bonding 2D-network (see text). Reaction energies upon adding one H_2O are given in kJ/mol. Color code as in Fig. 3.

In summary, the presented results of water adsorption on Fe_3O_4(111) at the initial stages, i.e. before the formation of ("multilayer") amorphous solid water sets in, show that water readily dissociates on the surface Fe_{tet}-O cation-anion pair to form two hydroxyl species. These act as anchors for molecular water adsorption resulting in dimer complexes which self-assemble into a (2×2) ordered structure. The formation of a long-range ordered water ad-layer is thermodynamically driven and includes cooperative formation of a hydrogen bonding network. The results further manifest a delicate balance that exists between water-surface and water-water interaction that determines stability of water species on oxide surfaces as recently demonstrated for the Cu_2O(111) surface solely on theoretical grounds.[16]

Experimental section

The experiments were performed in two UHV chambers with a background pressure below 3×10^{-10} mbar. All setups were equipped with standard facilities necessary to grow well-ordered F_3O_4(111) on a Pt(111) substrate. The quality of the films was checked by LEED showing sharp diffraction spots with low background intensity, and no other elements

beyond Fe and O were observed in Auger electron spectra (AES). Temperature programmed desorption (TPD) spectra were recorded using a quadrupole mass spectrometer (QMS, Hiden) having a gold-plated cone shield to minimize signals from the heating stage. IRA spectra were measured with a Bruker 66 ivs spectrometer. In the TPD/IRAS setup, water was dosed via calibrated molecular beam. In another (TPD) chamber, water was dosed using a directional doser.

The Fe_3O_4(111) films, with a thickness of about 5 nm, were grown on a Pt(111) substrate as described elsewhere. [3a-c, 4a] The first step includes formation of an FeO(111) monolayer film on the clean Pt(111) surface.[2a] This step is also used for calibration of the Fe deposition flux. The next step involves several (3-5) cycles of Fe deposition in amounts equivalent to 5-10 monolayers of FeO(111), followed by oxidation in ~ 10^{-6} mbar of O_2 at 900-940 K for ca. 10 min. Oxygen was pumped out at sample temperature around 500 K. In the final step, the films were oxidized at 930-940 K for 10 min. The "as prepared" films were inspected by LEED to ensure the formation of a uniform Fe_3O_4(111) film. Although the precise preparation parameters (Fe flux, oxidation temperature, time and oxygen pressure) used in each setup may slightly differ, all oxide films exhibited a sharp LEED pattern with a low background intensity. In addition, the samples prepared in different chambers showed similar TPD spectra of CO used as a probe molecule and of water that allowed cross-checking of the results. All adsorption measurements were performed at pressures below 5×10^{-10} mbar, and the samples were flashed in UHV to 900 K prior to water dosing performed with a directional doser in the TPD setup and molecular beam in the IRAS setup. TPD spectra were measured with a heating rate of 3 K/sec. IRA spectra were measured at grazing angle 8° with a resolution of 4 cm^{-1}.

DFT calculations were performed using the Vienna ab initio simulation package (VASP)[17] employing the projector augmented wave method to describe the electron ion interaction. The Perdew, Burke, Ernzerhof (PBE) [18] gradient-corrected exchange correlation functional [19] augmented with an effective Hubbard type U parameter (DFT+U using Dudarev's approach[20]) was used, with a U = 3.8 eV applied to the Fe 3d orbitals.[3f, 21] A plane wave energy cutoff of 800 eV is used. Brillouin zones of surface unit cells are sampled for integration by a (3×3×1) Γ-centered Monkhorst-Pack[22] *k*-point mesh.

Acknowledgements

This work has been supported by the Deutsche Forschungsgemeinschaft through SFB 1109, by the Fonds der Chemischen Industrie as well as by generous grants for computing time at the North-German Supercomputing Alliance in Berlin and Hannover. JP gratefully acknowledges the Stiftung Industrieforschung, Humboldt-Universität zu Berlin for financial support. FM thanks the International Max-Planck Research School "Functional Interfaces in Physics and Chemistry" for a fellowship.

References

[1] a) M. A. Henderson, *Surface Science Reports* **2002**, *46*, 1-308; b) P. A. Thiel, T. E. Madey, *Surf. Sci. Rep.* **1987**, *7*, 211-385.

[2] a) W. Weiss, W. Ranke, *Progr. Surf. Sci.* **2002**, *70*, 1-151; b) G. S. Parkinson, *Surf. Sci. Rep.* **2016**, *71*, 272-365; c) H. Kuhlenbeck, S. Shaikhutdinov, H.-J. Freund, *Chem. Rev.* **2013**, *113*, 3986-4034.

[3] a) M. Ritter, W. Weiss, *Surf. Sci.* **1999**, *432*, 81-94; b) S. K. Shaikhutdinov, M. Ritter, X. G. Wang, H. Over, W. Weiss, *Phys. Rev. B* **1999**, *60*, 11062-11069; c) A. Sala, H. Marchetto, Z. H. Qin, S. Shaikhutdinov, T. Schmidt, H. J. Freund, *Phys. Rev. B* **2012**, *86*, 155430; d) A. Kiejna, T. Ossowski, T. Pabisiak, *Phys. Rev. B* **2012**, *85*, 125414; e) J. Noh, O. I. Osman, S. G. Aziz, P. Winget, J.-L. Brédas, *Chem. Mat.* **2015**, *27*, 5856-5867; fX. Yu, C.-F. Huo, Y.-W. Li, J. Wang, H. Jiao, *Surf. Sci.* **2012**, *606*, 872-879; g) D. Santos-Carballal, A. Roldan, R. Grau-Crespo, N. H. de Leeuw, *Phys. Chem. Chem. Phys.* **2014**, *16*, 21082-21097.

[4] a)C. Lemire, R. Meyer, V. E. Henrich, S. Shaikhutdinov, H. J. Freund, *Surf. Sci.* **2004**, *572*, 103-114; b) P. Dementyev, K.-H. Dostert, F. Ivars-Barceló, C. P. O'Brien, F. Mirabella, S. Schauermann, X. Li, J. Paier, J. Sauer, H.-J. Freund, *Angew.Chem. Int. Ed.* **2015**, *54*, 13942-13946; c) X. Li, J. Paier, *J. Phys. Chem. C* **2016**, *120*, 1056-1065.

[5] X. Li, J. Paier, J. Sauer, F. Mirabella, E. Zaki, F. Ivars-Barceló, S. Shaikhutdinov, H. J. Freund, *J. Phys. Chem. B* **2017**. **DOI:** 10.1021/acs.jpcb.7b04228

[6] a) Y. Joseph, W. Ranke, W. Weiss, *J. Phys. Chem. B* **2000**, *104*, 3224-3236; b) T. Kendelewicz, P. Liu, C. S. Doyle, G. E. Brown Jr, E. J. Nelson, S. A. Chambers, *Surf. Sci.* **2000**, *453*, 32-46; c) Y. Joseph, C. Kuhrs, W. Ranke, M. Ritter, W. Weiss, *Chem. Phys. Lett.* **1999**, *314*, 195-202.

[7] a) R. S. Cutting, C. A. Muryn, D. J. Vaughan, G. Thornton, *Surf. Sci.* **2008**, *602*, 1155-1165; b) U. Leist, W. Ranke, K. Al-Shamery, *Phys. Chem. Chem. Phys.* **2003**, *5*, 2435-2441; c) K. Adib, G. G. Totir, J. P. Fitts, K. T. Rim, T. Mueller, G. W. Flynn, S. A. Joyce, R. M. Osgood Jr, *Surf. Sci.* **2003**, *537*, 191-204.

[8] S. L. Tait, Z. Dohnálek, C. T. Campbell, B. D. Kay, *J. Chem. Phys.* **2005**, *122*, 164707.

[9] S. Haq, J. Harnett, A. Hodgson, *Surf. Sci.* **2002**, *505*, 171-182.

[10] K. T. Rim, D. Eom, S.-W. Chan, M. Flytzani-Stephanopoulos, G. W. Flynn, X.-D. Wen, E. R. Batista, *J. Am. Chem. Soc.* **2012**, *134*, 18979-18985.

[11] a) B. Meyer, D. Marx, O. Dulub, U. Diebold, M. Kunat, D. Langenberg, C. Wöll, *Angew.Chem.Int. Ed.* **2004**, *43*, 6641-6645; b) Y. He, A. Tilocca, O. Dulub, A. Selloni,

U. Diebold, *Nat. Mater.* **2009**, *8*, 585-589; c) S. Kaya, J. Weissenrieder, D. Stacchiola, S. Shaikhutdinov, H. J. Freund, *J. Phys. Chem. C* **2006**, *111*, 759-764.
[12] R. Włodarczyk, M. Sierka, K. Kwapień, J. Sauer, E. Carrasco, A. Aumer, J. F. Gomes, M. Sterrer, H.-J. Freund, *J. Phys. Chem. C* **2011**, *115*, 6764-6774.
[13] a) C. Xu, D. W. Goodman, *Chem. Phys. Lett.* **1997**, *265*, 341-346; b) J. Heidberg, B. Redlich, D. Wetter, *Ber. Bunsen. Physik. Chem.* **1995**, *99*, 1333-1337; c) D. Ferry, A. Glebov, V. Senz, J. Suzanne, J. P. Toennies, H. Weiss, *J. Phys. Chem.* **1996**, *105*, 1697-1701.
[14] E. Zaki, F. Mirabella, F. Ivars-Barceló, J. Seifert, X. Li, J. Paier, J. Sauer, S. Shaikhutdinov, H. J. Freund, in prepration.
[15] J. D. Bernal, R. H. Fowler, *J. Phys. Chem.* **1933**, *1*, 515-548.
[16] C. Riplinger, E. A. Carter, *J. Phys. Chem. C* **2015**, *119*, 9311-9323.
[17] a) G. Kresse, J. Furthmüller, *Phys. Rev. B* **1996**, *54*, 11169-11186; b) G. Kresse, J. Furthmüller, *Comput. Mater. Sci.* **1996**, *6*, 15-50.
[18] J. P. Perdew, K. Burke, M. Ernzerhof, *Phys. Rev. Lett.* **1996**, ***77***, 3865-3868.
[19] a) P. E. Blöchl, *Phys. Rev.B* **1994**, *50*, 17953-17979; b) G. Kresse, D. Joubert, *Phys. Rev.B* **1999**, *59*, 1758-1775.
[20] S. L. Dudarev, G. A. Botton, S. Y. Savrasov, C. J. Humphreys, A. P. Sutton, *Phys. Rev.B* **1998**, *57*, 1505-1509.
[21] X. Yu, Y. Li, Y.-W. Li, J. Wang, H. Jiao, *J. Phys. Chem. C* **2013**, *117*, 7648-7655.
[22] H. J. Monkhorst, J. D. Pack, *Phys. Rev. B* **1976**, *13*, 5188-5192.

Ordered water layer at surface

F.Mirabella, E. Zaki, F.Ivars-Barceló, X. Li, J.Paier,* J.Sauer, S. Shaikhutdinov,* H.-J. Freund

_____ Page – Page

Cooperative formation of long-range ordering in water ad-layers on Fe_3O_4(111)

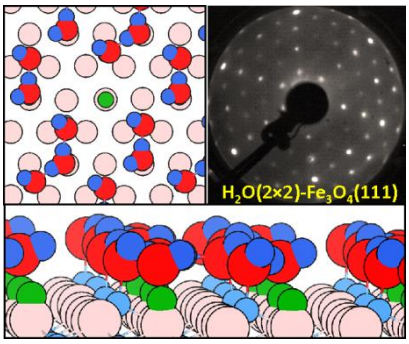

We provide experimental and theoretical results showing that water readily dissociates on Fe_{tet} sites to form two hydroxo species which act as an anchor for water molecules which self-assembles into an ordered (2×2) structure. Water ad-layer ordering is rationalized in terms of a cooperative effect induced by a hydrogen bonding network.